

1 **Forward genetic screens identified mutants with defects in trap morphogenesis**

2 **in the nematode-trapping fungus *Arthrobotrys oligospora***

3 Tsung-Yu Huang^{*, †}, Yi-Yun Lee^{*, ‡}, Guillermo Vidal-Diez de Ulzurrun^{*},

4 Yen-Ping Hsueh^{*, †, ‡, §}

5 ^{*}Institute of Molecular Biology, Academia Sinica, Nangang, 128 Academia Road,

6 Section 2, Nangang, Taipei, Taiwan

7 [†]Department of Biochemical Science and Technology, National Taiwan University No.

8 1, Sec. 4, Roosevelt Road, Taipei, Taiwan

9 [‡]Department of Genome and Systems Biology Degree Program, National Taiwan

10 University and Academia Sinica, Taipei 106, Taiwan

11

12

13

14

15

16 [§] Corresponding author

17 Institute of Molecular Biology

18 Academia Sinica

19 128 Academia Road, Section 2, Nangang,

20 Taipei, 115 Taiwan

21 Email: pinghsueh@gate.sinica.edu.tw

22 Phone: 886-2-2789-9313

23 **Abstract**

24 Nematode-trapping fungi (NTF) are carnivorous fungi that prey on nematodes under
25 nutrient-poor conditions via specialized hyphae that function as traps. The molecular
26 mechanisms involved in the interactions between nematode-trapping fungi and their
27 nematode prey are largely unknown. In this study, we conducted forward genetic
28 screens to identify potential genes and pathways that are involved in trap
29 morphogenesis and predation in the NTF *Arthrobotrys oligospora*. Using Ethyl
30 methanesulfonate and UV as the mutagens, we generated 5552 randomly-
31 mutagenized *A. oligospora* strains and identified 15 mutants with strong defects in
32 trap morphogenesis. Whole genome sequencing and bioinformatic analyses revealed
33 mutations in genes with roles in signaling, transcription or membrane transport that
34 may contribute to the defects of trap morphogenesis in these mutants. We further
35 conducted functional analyses on a candidate gene, *YBP-1*, and demonstrate that
36 mutation of that gene was causative of the phenotypes observed in one of the mutants.
37 The methods established in this study might provide helpful insights for establishing
38 forward genetic screening methods for other non-model fungal species.

39

40

41

42 **Introduction**

43 Model organisms have contributed enormously to unraveling the fundamental
44 principles of biology. However, in some cases, model organisms might not be the most
45 ideal investigatory system and studies on non-model species could better answer
46 specific questions (Russell et al., 2017). Fortunately, by adopting increasingly more
47 affordable and advanced next-generation sequencing technologies, intensive study at
48 molecular and cellular levels of non-model species is now possible (Ellegren and
49 evolution, 2014).

50 The fungal kingdom harbors rich biodiversity, with an estimated ~12 million
51 species (Wu et al., 2019). Apart from for several model yeast and filamentous species,
52 particularly pathogenic ones, we have very limited molecular or cellular knowledge on
53 the vast majority of fungi. Fungi occur in essentially all habitats on Earth, and many
54 species have evolved unique traits. For example, many species of Orbiliaceae
55 (Ascomycota) are predatory fungi that prey on nematodes when local nutrients are
56 scarce by means of specialized mycelial structures. More than 200 of these nematode-
57 trapping fungi (NTF) have been described to date, with *Arthrobotrys oligospora* being
58 the best studied species (Nordbring-Hertz et al., 2011). *A. oligospora* is known to
59 eavesdrop on nematode ascaroside pheromones to trigger trap morphogenesis and to
60 produce volatile compounds mimicking food and sex cues that lure nematodes, and

61 predatory abilities among natural populations of this species can vary considerably
62 (Hsueh et al., 2017; Hsueh et al., 2013; Yang et al., 2020).

63 NTF hold great promise as biocontrol agents to combat plant-parasitic nematodes,
64 which have been estimated to cause USD\$ 80 million in crop loss annually (Gray, 1983;
65 Lopez-Llorca et al., 2007; Wang et al., 2015). However, since we know little about their
66 biology and the cellular/molecular mechanisms governing the switch from saprophytic
67 to predatory lifestyles, the full nematocidal potential of NTF cannot yet be harnessed.
68 Nematode-derived cues are key signals triggering the switch to a predatory lifestyle
69 switch in NTF (Hsueh et al., 2013). Consequently, signaling pathways could be
70 anticipated to play vital roles in this lifestyle switch. Indeed, a few such genes have
71 been demonstrated as necessary for trap morphogenesis in *A. oligospora*. These
72 include the mitogen-activated protein kinase (MAPK), Slf2, which is involved in the
73 cell wall integrity signaling pathway in yeast (Zhen et al., 2018), a pH-sensing receptor,
74 palH, that functions in the pH signal transduction pathway, and a NADPH oxidase,
75 NoxA, that controls ROS signaling responses in *A. oligospora* (Li et al., 2019; Li et al.,
76 2017). More recently, it has been demonstrated that the G protein beta subunit, Gpb1,
77 is required for the predatory lifestyle transition in *A. oligospora* (Yang et al., 2020).
78 Nevertheless, more intensive study is needed to gain further insight into the
79 mechanisms governing these inter-kingdom predator-prey interactions.

80 In this study, we have established methods for conducting forward genetic screens
81 of *A. oligospora*. By applying this approach together with whole genome sequencing,
82 we demonstrated that it is possible to identify genes playing important roles in trap
83 morphogenesis and, further, to unveil the causative mutation in a mutant that failed to
84 develop traps without the need to conduct genetic crosses. Our work illustrates that it
85 is feasible to conduct random mutagenesis on a fungal species for which the sexual
86 cycle has not been well studied in the laboratory and to identify causative mutations for
87 phenotypic traits. Through our forward genetic screens, we have identified novel
88 players necessary for the predatory lifestyle of *A. oligospora*.

89

90 **Materials and methods**

91 **Strains, media, culture conditions**

92 *Arthrobotrys oligospora* strain TWF154 was used in this study, a wild isolate we
93 have sampled in Taiwan. Genomic data on this strain can be accessed from the National
94 Center for Biotechnology Information GenBank under accession number
95 SOZJ000000000 (Yang et al., 2020). All corresponding knockout mutants were obtained
96 in a *ku70* strain background. Our use of *ku70* protoplasts increased the efficiency of
97 targeted gene knockout as cells may fail to enter the nonhomologous end-joining
98 pathway without Ku70 protein, resulting in greater likelihood of undergoing

99 homologous recombination during DNA repair.

100 We used potato dextrose agar (PDA) and low nutrient medium (LNM) as fungal
101 solid media, whereas yeast nitrogen base without amino acids (YNB) and potato
102 dextrose broth (PDB) acted as liquid media. We used *Caenorhabditis elegans* wild-type
103 strain N2 as nematode prey, which were maintained on nematode growth media (NGM)
104 plates with *Escherichia coli* OP50 as food. All cultures were incubated at 25 °C.

105 **Mutagenesis**

106 TWF154 was cultured on PDA for 5 days and the hyphae and spores were
107 collected into 50 ml PDB for liquid culture. After culturing for 2 days at 25 °C, the
108 liquid culture was blended and then treated with 10 ml Vino Taste Pro (80 mg/ml in
109 MN buffer) and chitinase for 8-10 h at 30 °C and 200 rpm in an incubator to digest
110 fungal cell walls. Digested cells were then filtered through two layers of sterile
111 miracloth (EMD Millipore) and washed with sterile STC buffer (1.2 M D-Sorbitol, 10
112 mM Tris-HCl (pH 7.5), 50 mM CaCl₂).

113 Next, we spread 5×10^4 protoplasts onto a regeneration plate and subjected them to
114 a treatment of either 6 sec of 15 W UV or 12 µg/ml ethyl methanesulfonate (EMS) to
115 cause random mutations in the genomes. Plates were then cultured under dark
116 conditions at 25 °C to prevent DNA repair. Any colonies formed were then further
117 inoculated onto PDA 48-well plates.

118 **Genetic screen on mutants with trapping defects**

119 To screen out mutants exhibiting defects in trapping *C. elegans*, colonies that grew
120 after mutagenesis were inoculated onto LNM 48-well plates. Colonies in each well were
121 then exposed overnight to thirty specimens of N2, and those exhibiting weak trapping
122 ability after 24 hours were selected for rescreening. The rescreening process was
123 conducted on 5-cm LNM plates on which mutant fungal lines were exposed to ~100
124 N2. By rescreening we could exclude false positive mutants, resulting in more accurate
125 phenotyping of trapping defects.

126 **Trap quantification**

127 To quantify trap formation, fungal strains were inoculated onto fresh 3-cm LNM
128 plates and grown for 3 days. Then, thirty L4 larval-stage N2 were added to the plate
129 and washed away after 6 hours. Fungal cultures were incubated at 25 °C and we
130 calculated number of traps from half of the plate after 24 hours and presented the results
131 in traps/cm².

132 **Visualization of trap morphology**

133 Fungal strains were inoculated onto 12-well LNM plates, and 0.1% SCRI
134 Renaissance 2200 (SR2200; a dye that binds to beta-1,3-glucan) was added to the
135 medium. Thirty L4 larval-stage N2 were added to the plates and 24-h later the plates
136 were imaged at 40x magnification using an Axio Observer Z1 system.

137 **Whole-genome sequencing analysis**

138 Genomic DNA extracted from 16 mutants was subjected to whole genome
139 sequencing using an Illumina sequencing system. Approximately 18 million reads were
140 trimmed to generate a 250 base-pair (bp) library and a paired-end sequencing protocol
141 enabled us to derive more accurate sequencing results.

142 For data analysis, index files from the TWF154 reference genome (Yang et al.,
143 2020) were created using samtools (Li, 2011) and bwa (Li and Durbin, 2009). Then, we
144 trimmed the adaptors with Trimmomatic (Bolger et al., 2014) and filtered out low-
145 quality reads from each of the sequenced mutants. Trimmed reads from each mutant
146 were aligned to the reference genome using bwa-mem (Li, 2013) and converted to
147 BAM files. Next, we used Picard (Picard toolkit., 2019) to identify duplicates, and
148 GATK (Poplin et al., 2017) was employed for SNV (single nucleotide variation) and
149 INDEL (insertion/deletion) calling in each file. Two separate files of all variants were
150 then generated, one of which contained only INDELS and the other only SNPs. To focus
151 on the most relevant mutations, the SNP and INDEL files were filtered using gatk
152 VariantFiltration and gatk SelectVariants (Poplin et al., 2017) with the following criteria:
153 $QD < 2.0$, $MQ < 40.0$, $QUAL < 100$, $MQRankSum < -12.5$, $SOR > 4.0$, $FS > 60.0$,
154 $ReadPosRankSum < -8.0$. The mutations were annotated in ANNOVAR (Wang et al.,
155 2010) by comparing the files to the reference genome. To narrow down potential

156 candidate genes, we focused on exonic regions and excluded synonymous mutations as
157 well as mutations occurring more than twice among the mutants. Genes potentially
158 contributing to trapping defects were validated by gene ontology prediction.

159 **Transformation**

160 We placed 10^6 protoplasts on ice in a 50-ml centrifuge tube for 30 min with 5 μ g
161 of knockout cassette DNA (see below). Then, five volumes of PTC buffer (40%
162 polyethylene glycol 3350, 10 mM Tris-HCl (pH 7.5), 50 mM CaCl_2) was added and
163 gently mixed by inverting the tube. After multiple inversions, the tube was kept at room
164 temperature for 20 min. Lastly, protoplasts were mixed with regeneration agar (3%
165 acid-hydrolyzed casein, 3% yeast extract, 0.5 M sucrose, 10% agar) and 200 μ g/ml
166 Nourseothricin Sulfate (clonNAT).

167 **Construction of gene knockout cassettes**

168 Gene knockout cassettes consisted of three fragments, i.e., 2-kb homologous
169 sequences of the 5' and 3' untranslated region (UTR) of the target gene flanking a
170 nourseothricin acetyltransferase gene (*NATI*). Two homologous sequences were
171 designed to overlap with the *NATI* gene. The three fragments were amplified separately,
172 and these were then conjoined into complete cassettes by amplifying using nested
173 primers targeting to both ends of the cassette.

174 **Confirmation of gene knockouts in mutants**

175 To confirm knockout by PCR, we used two pairs of primers, each pair having one
176 primer in the DNA flanking the targeted region to be knocked out and one in the *NATI*
177 gene, and amplified both intervening junctions. Another PCR reaction, using the two
178 primers within the targeted region, was also performed to confirm the absence of the
179 knockout gene, thereby ruling out the possibility of a duplication event.

180 Moreover, Southern blots were conducted on transformants to confirm knockout
181 and to check if there had been any ectopic integrations of the drug-resistance cassette
182 elsewhere in the genome.

183 **Rescue assay on EYR41_001410 in the TWF1042 mutant**

184 Constructs were amplified from 2-kb upstream to 1-kb downstream of the
185 EYR41_001410 sequence and fused with a G418 (Geneticin) drug cassette. We
186 transformed 5 μg of constructs into 2.5×10^5 of TWF1042 protoplasts and cultured them
187 with 200 $\mu\text{g}/\text{ml}$ of G418. Any resulting colonies were inoculated onto PDA plates with
188 150 $\mu\text{g}/\text{ml}$ G418 for confirmation.

189

190

191

192

193

194 **Results**

195 **Forward genetic screening identifies *A. oligospora* mutants with trapping defects**

196 To establish a protocol for forward genetic screens that could identify genes
197 involved in the trapping process of NTF, we optimized the mutagenesis conditions for
198 a lethal dose (LD₅₀) using EMS- or UV-treated protoplasts (6 seconds of 15 W UV or
199 12 µg/ml EMS). Then, the resulting 5552 mutagenized clones (1560 from UV- and 3992
200 from EMS-based mutagenesis) were isolated onto 48-well plates. We screened these
201 5552 mutant lines twice and identified 15 that exhibited defects in capturing *C. elegans*
202 (Fig. 1). Unlike control wild-type strain TWF154, which formed numerous traps and
203 captured all 30 *C. elegans* within 12 hours of our nematode-trapping assay, many live
204 nematodes were still crawling over the mutant strains within the same timeframe and
205 the mutants presented few or no traps (Fig. 2). Interestingly, some of the mutants
206 exhibited delayed trap formation, with traps eventually being formed 24 hours after
207 exposure to *C. elegans* (Supplementary figure 1). In summary, all of the mutants
208 isolated from our genetic screens exhibit defects in trap development in the presence of
209 nematode prey.

210 **Phenotypic characterization of the 15 mutants exhibiting trapping defects**

211 We further quantified their trap-forming capabilities in all 15 mutants that we had
212 isolated from the genetic screens. We found that all mutant lines developed fewer traps

213 relative to wild-type upon exposure to the same number of nematode prey, with trap
214 morphogenesis being completely abolished in six of the mutant lines (Fig. 3A).

215 We then examined the morphology of the traps developed by these 15 mutants.
216 The traps generated by wild-type *A. oligospora* are three-dimensional structures
217 consisting of several loops of hyphae of varying size. In contrast, the traps formed by
218 the mutants tended to have abnormal morphologies, either because the loops failed to
219 fuse or the loops were irregularly shaped (Fig. 3B). It has been demonstrated previously
220 that intercellular communication is critical for trap formation (Nordbring-Hertz et al.,
221 2011; Youssar et al., 2019), so these phenotypes could result from deficient
222 communication between hyphal cells or defects in initiating trap morphogenesis. Many
223 of the mutants exhibited vegetative hyphal protrusions in response to nematode
224 presence but were incapable of completing trap morphogenesis, some developed
225 rudimentary traps, and others completely lacked any trap-like structures (Fig. 3B).

226 Next, we tested if these mutants exhibit general growth defects by culturing them
227 on the rich medium potato dextrose agar (PDA). Four out of fifteen mutant lines showed
228 growth defects relative to the wild-type strain, suggesting that these particular mutant
229 lines harbor mutations in genes that may play pleiotropic roles in general growth (Fig.
230 3C). The remaining 11 mutants displayed no overt growth differences compared to
231 wild-type, implying that the mutated genes might play more specific roles in *A.*

232 *oligospora* trap formation.

233 **Whole genome sequencing analysis of the 15 mutant lines identifies potential**
234 **candidate genes involved in trap morphogenesis**

235 To identify the mutations in the genomes of the 15 mutant lines, we conducted
236 whole genome sequencing and remapped all sequencing data to the wild-type TWF154
237 reference genome. On average, 2700 mutations encompassing noncoding and coding
238 sequences were identified in each of these mutants, but many of those mutations were
239 common to all mutant lines, perhaps representing background mutations between the
240 mutagenized clone and the original sequenced clone (Supplementary figure 2). Such
241 mutations were ruled out from further analyses (Table 1). Of the 10-89 mutations
242 remaining in each of the mutant lines, we focused on those occurring within exonic
243 sequences to further refine the group of candidate genes (Table 1). In certain mutant
244 lines, such as TWF1037, TWF1042, TWF1046 and TWF1073, we identified mutations
245 in exons of more than 20 genes, whereas for two mutant strains (TWF1033 and
246 TWF1034) we did not identify any coding genes with mutations, indicating that the
247 mutations that caused trapping defects in these two latter mutants likely occur in
248 noncoding regions of the genome.

249 In the final step of our mutation selection process, we excluded genes having
250 synonymous mutations, and selected genes that gained a misplaced stop codon for

251 further functional studies (Table 1). We identified loss-of-function mutations, such as
252 stop gain mutations, frameshift indels, and nonsynonymous SNV, among the mutants
253 (Fig. 4). We used gene ontology analysis to predict the functions of the mutated genes
254 identified from our sequencing analyses and discovered that they play roles in signaling,
255 transcription or membrane transport (Supplementary Table 2). Together, these analyses
256 have revealed a set of genes that, when mutated, may contribute to the phenotype of
257 impaired trap formation and nematode predation.

258

259 **Frameshift indel mutation in gene EYR41_001410 induces phenotypic defects in**
260 **the TWF1042 mutant strain**

261 To further assess identified candidate mutated genes and establish which mutations
262 were causative for the phenotypes observed in the mutants, we focused on mutant strain
263 TWF1042 that had mutations in seventeen candidate genes, including three frameshift
264 indel mutations (Fig. 4). Reasoning that these three frameshift mutations likely
265 abolished the respective protein function, we examined our gene ontology predictions
266 and discovered that one putative sequence had a protein kinase domain
267 (EYR41_005093), another had a YAP-binding/ALF4/Glomulin domain
268 (EYR41_001410), and the other was of unknown function (EYR41_008629). In
269 *Saccharomyces cerevisiae*, YAP-binding proteins function in responses to oxidative

270 stress (Gulshan et al., 2004). In *Arabidopsis thaliana*, Aberrant root formation protein
271 4 (Alf4) is involved in the initiation of lateral root formation (DiDonato et al., 2004).
272 Deletion of the *Glomulin* gene was reported to affect differentiation in vascular smooth
273 muscle cells in mouse (Arai et al., 2003). Given these diverse biological functions of
274 the YAP-binding/ALF4/Glomulin protein family, we hypothesized that the protein
275 encoded by *EYR41_001410* in *A. oligospora*, which we have named *YPBI* (YAP-
276 binding protein 1), might play an important role in hyphal growth in this fungus. *YPBI*
277 appears to be a rapidly-evolving gene. It shares ~70% protein sequence identity among
278 NTF, but only ~20% protein sequence identity with other ascomycetes (Fig. 5A).
279 Consequently, the YAP-binding protein gene family may play diverse roles in a variety
280 of fungal species.

281 To study the function of *YPBI*, we constructed a gene deletion mutant via
282 homologous recombination and examined the phenotypes of the resulting *ypb1* mutant.
283 We found that *ypb1* displayed phenotypes similar to those exhibited by our randomly
284 mutagenized strain, TWF1042, including slow growth, lack of conidiation and severe
285 defects in trap formation (Fig. 5B and C). These results indicate that the frameshift
286 insertion mutation in *YPBI* likely caused the phenotypic defects observed in strain
287 TWF1042. To validate that supposition, we expressed the wild-type allele of *YPBI*
288 under its endogenous promoter in TWF1042 to examine if addition of a wild-type copy

289 of *YPBI* could rescue the phenotypic defects displayed by TWF1042. Indeed, addition
290 of the wild-type *YPBI* allele to TWF1042 complemented its defects in trap formation,
291 growth, and conidiation, demonstrating that the frameshift insertion mutation of *YPBI*
292 caused the phenotypic defects observed for TWF1042 (Fig. 5C).

293

294 **Discussion**

295 In this study, we established a protocol to conduct forward genetic screens in the
296 NTF, *A. oligospora*. We used EMS or UV to mutagenize protoplasts and screened out
297 fifteen mutants exhibiting defects in trap formation. Subsequent whole genome
298 sequencing identified candidate genes harboring mutations in these mutants. Finally,
299 we demonstrate that a frameshift mutation of the YAP-binding/ALF4/Glomulin
300 domain-containing gene, *YPBI*, caused the nematode-trapping defects observed in one
301 of the randomly-mutagenized mutant strains, TWF1042.

302 Although we identified 15 mutants with defects in trap morphogenesis from our
303 genetic screens, we consider the success rate in isolating mutants to be low (15 out of
304 ~5,500 mutagenized clones), and our screens were far from achieving mutagenesis
305 saturation. We believe that two factors contributed to this result. First, mutagen dosages
306 may have been too light and, second, some of our mutagenized clones could be
307 heterokaryons of mixed genetic backgrounds, which could mask phenotypes caused by

308 mutations. We purposely used lower mutagen dosages because laboratory methods for
309 conducting genetic crosses of *A. oligospora* have yet to be established. If too many
310 mutations had been generated in the background genome, it would be challenging to
311 identify the mutations causing the observed phenotypes without undertaking genetic
312 mapping analyses. Since the hyphae of *A. oligospora* contain multiple nuclei, it is
313 possible that a small proportion of the protoplasts we generated and mutagenized
314 harbored more than one nucleus, and it is also possible that some of the single mycelium
315 colonies we isolated had fused with a neighboring colony of a different genetic
316 background. Both scenarios could lead to heterokaryons occurring in our *A. oligospora*
317 mutant libraries.

318 We believe that to make forward genetic screening even more applicable to NTF
319 study, laboratory genetic crosses must be established. Doing so would enable
320 significantly higher mutagen dosages to be applied, rendering mutant identification
321 more efficient. In summary, we have established a method for conducting random
322 mutagenesis in a non-model fungus, followed by resequencing of the mutants to
323 identify candidate genes contributing to observed phenotypes. We have revealed that
324 YBP1 plays a critical role in the physiology and development of *A. oligospora* and also
325 identified several other candidate genes in which mutations might cause defects in trap
326 morphogenesis. We envisage that our methodology could facilitate future genetic

327 studies in other enigmatic fungi.

328 **Acknowledgments**

329 The authors thank the IMB genomic core for conducting Illumina sequencing and

330 John O'Brien's comments on the manuscript. This work was supported by Academia

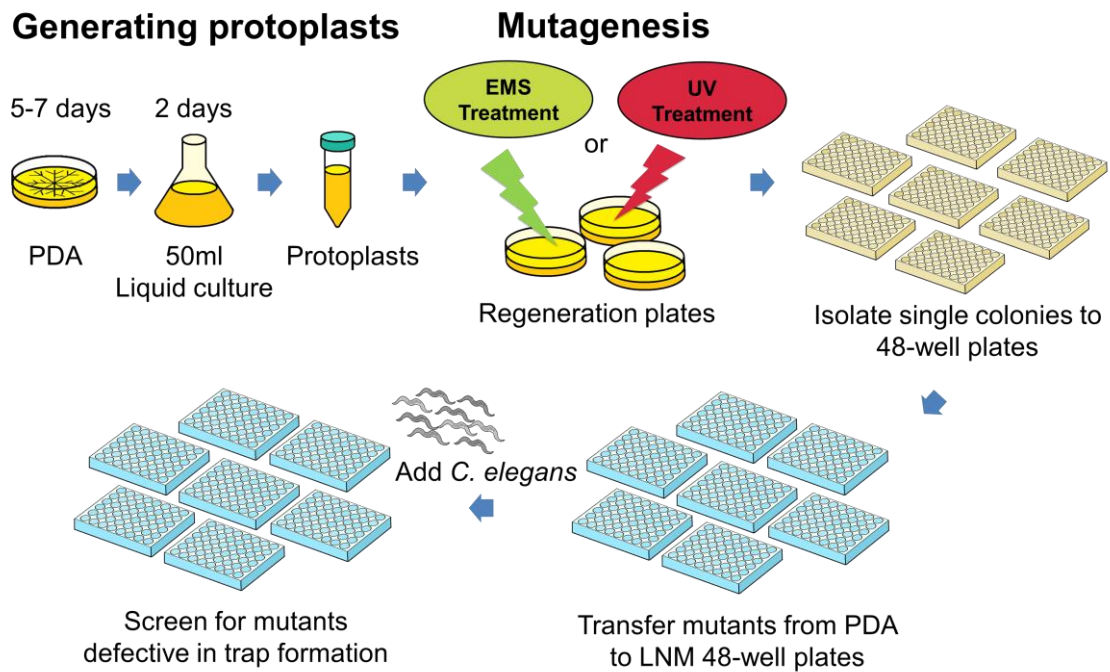
331 Sinica Career Development Award AS-CDA-106-L03 and Taiwan Ministry of Science

332 and Technology grant 106-2311-B-001-039-MY3 to YPH.

333

334

335 **Figures**



336

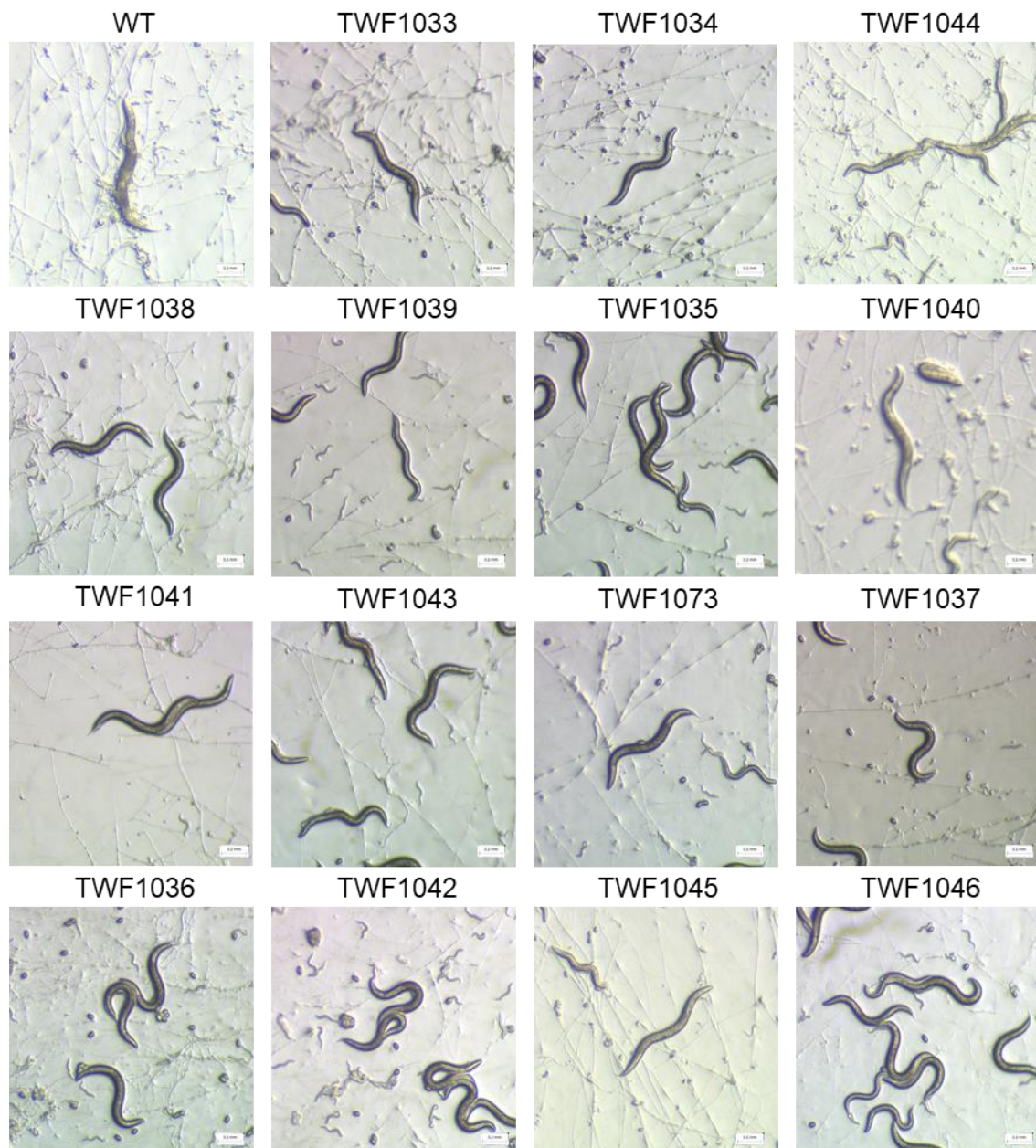
337 Fig. 1 Schematic of our workflow for random mutagenesis and forward genetic screening of *A.*

338 *oligospora*. Protoplasts were acquired from PDB liquid culture and were subsequently treated

339 with EMS or UV for mutagenesis. The resulting colonies were separated out into 48-well PDA

340 plates and screened on LNM plates. Mutants with trapping defects were selected after a

341 rescreening process.



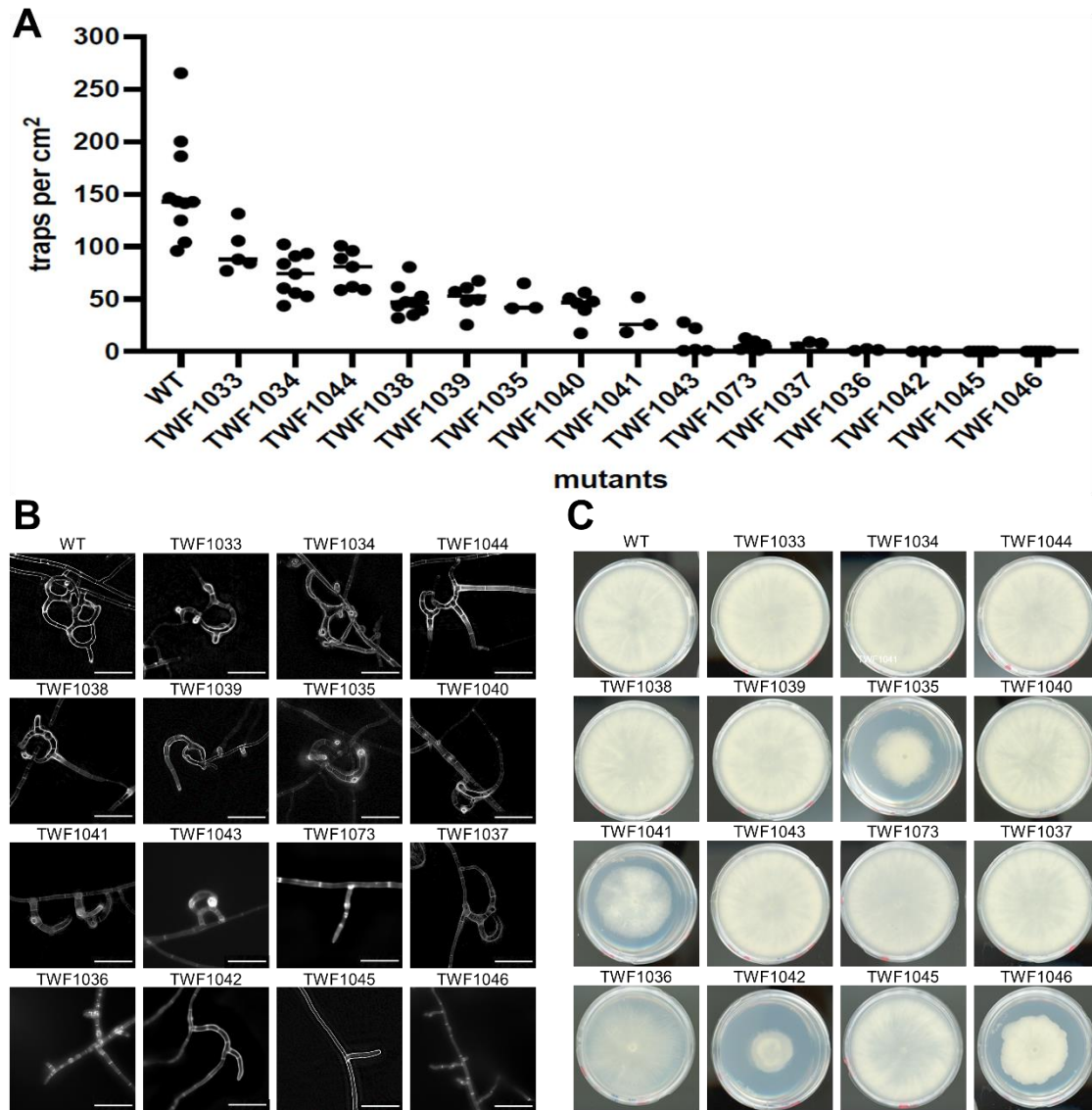
342

343 Fig. 2 Random mutagenesis and genetic screening identified 15 *A. oligospora* mutants

344 with defects in trap morphogenesis. All images are of *A. oligospora* upon 12-h exposure

345 to N2 *C. elegans*.

346



347

348 Fig. 3 Phenotypic characterization of the 15 mutants identified from our forward genetic

349 screen. (A) Quantification of trap numbers induced by *C. elegans* for the WT and 15

350 mutant lines. (B) Microscopic analyses of trap morphology for WT and the 15 mutant

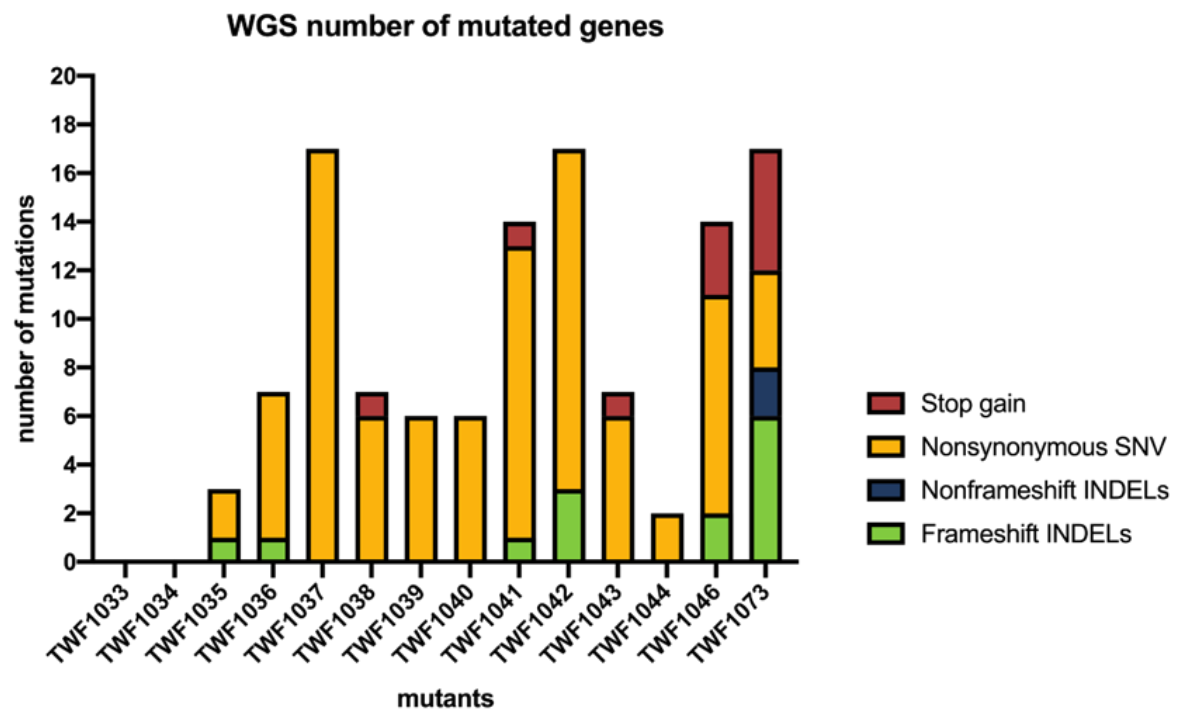
351 lines. Bars, 50 μ m. (C) Growth of WT and 15 mutant lines on PDA plates (5-cm diameter)

352 by day 5.

353 Table 1. Summary of numbers of mutations (after filtering out common mutations) among the 15 mutant lines, as identified by whole
 354 genome sequencing. Exonic mutations encompass frameshift indels, non-frameshift indels, non-synonymous, synonymous and stop-gain
 355 mutations. Indel, insertion/deletion; SNV, single nucleotide variation.

Mutant	Upstream	Downstream	Intergenic	Intronic	5'UTR	3'UTR	Exonic	Frameshift indels	Non-frameshift indelss	Non-synonymous SNV	Synonymous SNV	Stop-gain	Total
TWF1033	1	3	6	1	0	0	0	0	0	0	0	0	11
TWF1034	1	2	5	2	0	0	0	0	0	0	0	0	10
TWF1035	4	4	7	4	1	0	3	1	0	2	0	0	23
TWF1036	5	8	9	2	2	4	8	1	0	6	1	0	38
TWF1037	10	6	28	5	9	7	24	0	0	18	6	0	89
TWF1038	5	6	8	7	2	2	12	0	0	6	5	1	42
TWF1039	2	5	10	0	2	1	10	0	0	7	3	0	30
TWF1040	5	7	5	1	2	1	10	0	0	7	3	0	31
TWF1041	3	5	9	4	4	1	17	1	0	12	4	1	43
TWF1042	13	3	15	8	4	0	26	3	0	14	9	0	69
TWF1043	6	7	11	10	2	2	12	0	0	6	5	1	50
TWF1044	5	2	6	7	4	2	3	0	0	2	1	0	29
TWF1046	14	3	12	11	9	5	26	2	0	9	12	3	80
TWF1073	28	6	4	6	14	4	22	9	3	4	1	5	84

356

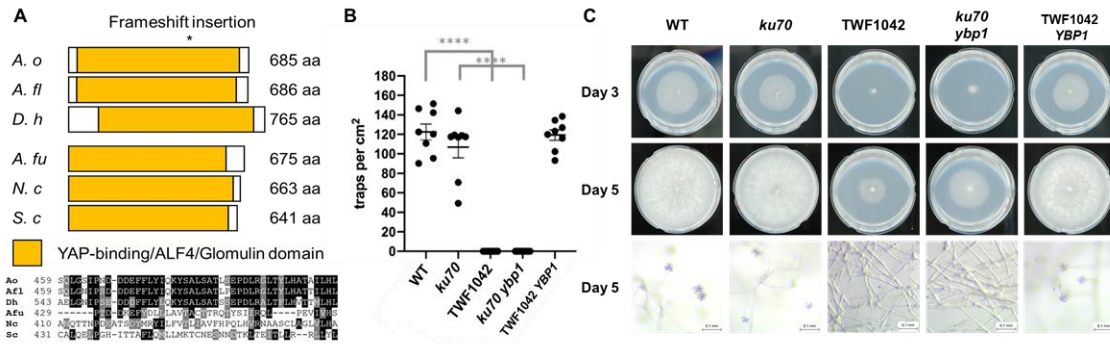


357

358 Fig. 4 Numbers of mutated genes (after filtration procedures) in each mutant.

359 Different colors represent different types of exonic mutations (excluding

360 synonymous mutations).



361

362 Fig. 5. Mutations in *YBP1* cause the phenotypic defects in growth, trap morphogenesis

363 and conidiation observed in the randomly-mutagenized strain TWF1042. (A)

364 Schematic representation of the domain structure and partial sequence alignment of *A.*

365 *oligospora* YBP1 and related fungal homologs. *A. oligospora* (*A. o.*), *Arthrobotrys*

366 *flagrans* (*A. fl.*), *Dactylellina haptotyla* (*D. h.*), *Aspergillus fumigatus* (*A. fu.*), *Neurospora*

367 *crassa* (*N. c.*), *Saccharomyces cerevisiae* (*S. c.*). Asterisk represents the site where

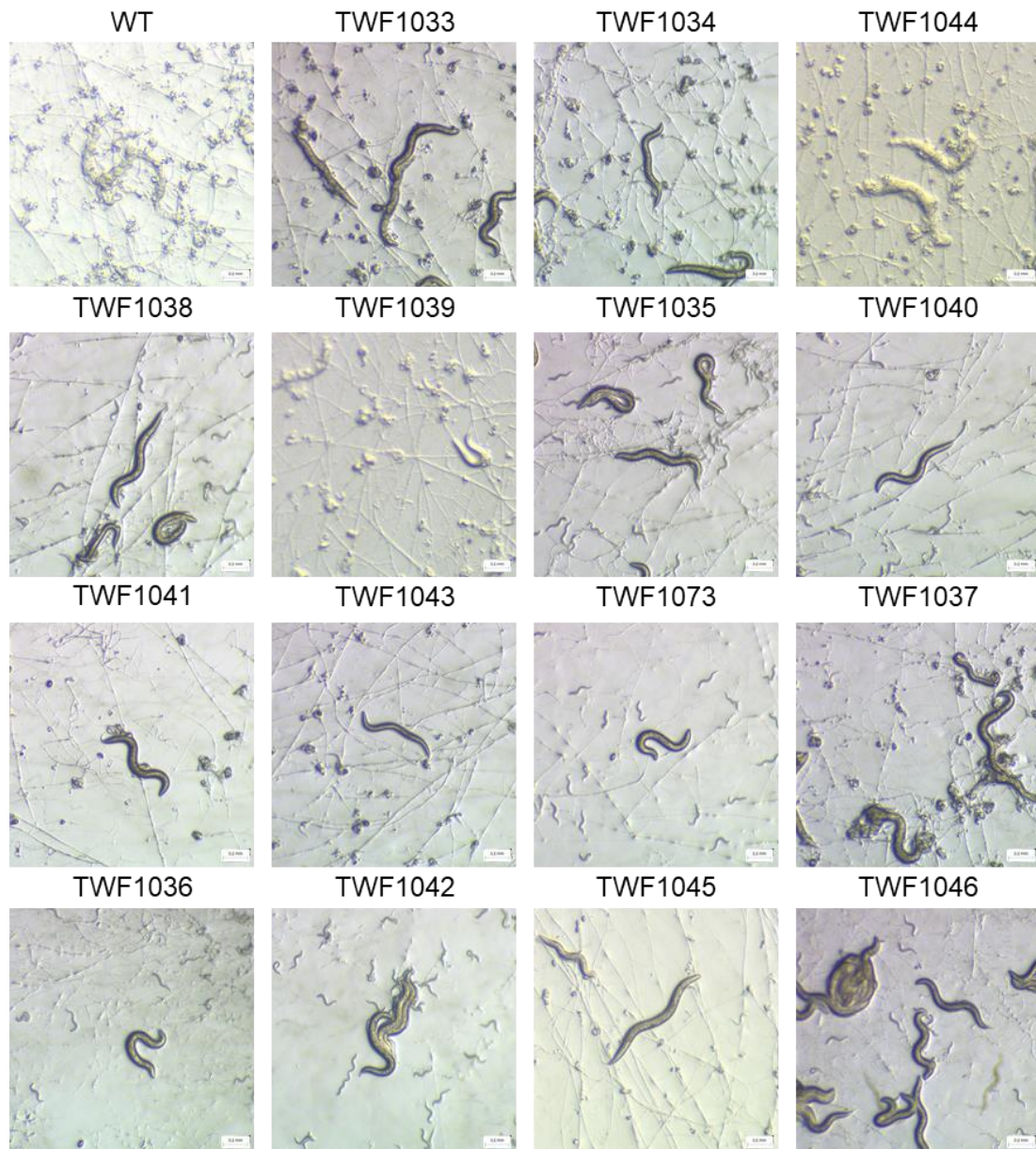
368 frameshift insertion was found. (B) Quantification of trap numbers induced by *C.*

369 *elegans* presence for the WT, *ku70*, TWF1042, *ku70 ybp1*, and a TWF1042-*YBP1*

370 rescue strain. (C) Representative images of growth (day 3), aerial hyphae (day 5), and

371 conidiation (day 5) for the WT, *ku70*, TWF1042, *ku70 ybp1*, and TWF1042-*YBP1*

372 rescue strain. Colonies were grown on PDA plates (5-cm diameter).



373

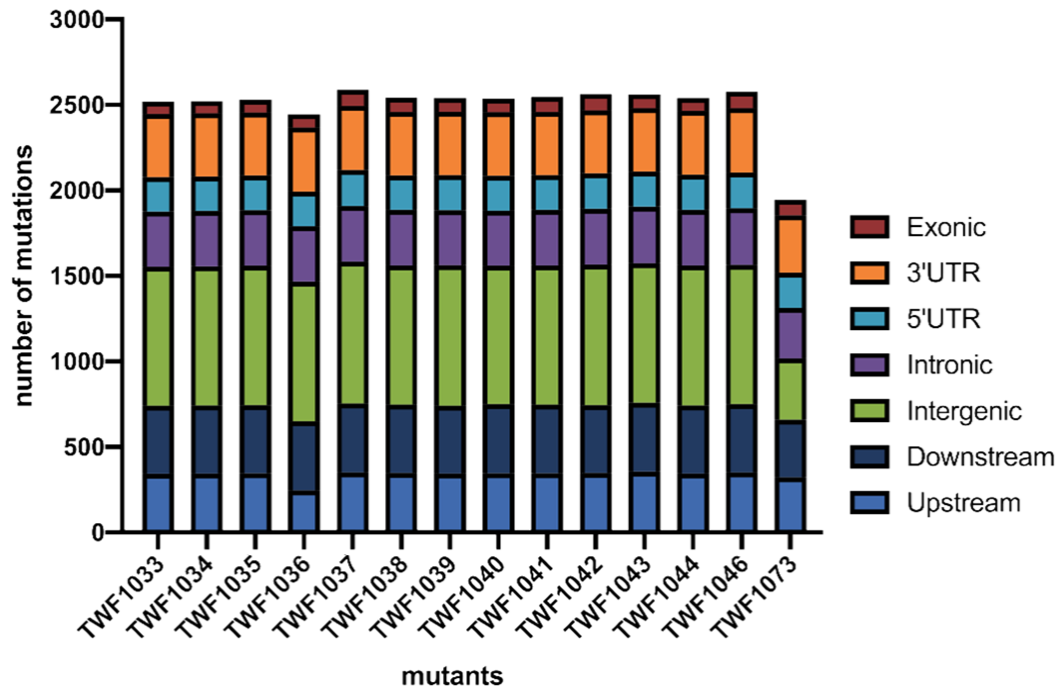
374 Supplementary fig.1 Random mutagenesis and forward genetic screening identified 15

375 mutants with defects in capturing *C. elegans*. *C. elegans* were paralyzed and dead in WT

376 group but there were still living worms in mutants. Micrographs were captured at the 24-

377 h time-point. Some mutants showed delayed trap formation and others still failed to form

378 traps.



379

380 Supplementary fig. 2 Total mutations annotated for each mutant. Different types of

381 mutation are individually colored.

382 Supplementary Table 2. Information on selected genes (after filtration procedures) to conduct targeted gene knockout. “Chr” column presents the
383 chromosome that the mutations were located. “Start” and “End” column present the exact sites where the mutations were found. “Ref” and “Alt”
384 column present the nucleotides from reference genome and mutants respectively. “Exonic Func.” presents the type of the mutations. “GO terms”
385 presents the predicted function of the gene.

Mutant	Gene	Chr	Start	End	Ref	Alt	Exonic Func.	GO terms
TWF1035	EYR41_000049	scaffold_1	149046	149046	-	TCTGTAA	frameshift insertion	Creatinase/aminopeptidase-like
TWF1036	EYR41_003391	scaffold_2	2818724	2818724	A	G	nonsynonymous SNV	Major facilitator, sugar transporter-like
TWF1036	EYR41_009094	scaffold_6	793179	793179	T	A	nonsynonymous SNV	Zinc finger, CCCH-type superfamily
TWF1037	EYR41_002645	scaffold_2	399109	399109	T	A	nonsynonymous SNV	F-box-like domain superfamily
TWF1037	EYR41_008023	scaffold_5	1235392	1235392	T	A	nonsynonymous SNV	Protein kinase domain
TWF1038	EYR41_005196	scaffold_3	1505468	1505468	-	TA	stop-gain	MFS transporter superfamily
TWF1038	EYR41_011609	scaffold_8	2469219	2469219	T	A	nonsynonymous SNV	Cytochrome P450, E-class, group I
TWF1039	EYR41_008594	scaffold_5	3072546	3072546	G	A	nonsynonymous SNV	Zinc finger, GATA-type;zinc finger, GATA-type
TWF1041	EYR41_005971	scaffold_3	3955532	3955532	A	T	stop-gain	Copper amine oxidase, catalytic domain
TWF1042	EYR41_001410	scaffold_1	4520093	4520093	-	TTCCGACGAATTT	frameshift insertion	YAP-binding/ALF4/Glomulin
TWF1042	EYR41_005093	scaffold_3	1186858	1186858	-	T	frameshift insertion	Protein kinase domain
TWF1042	EYR41_008629	scaffold_5	3181771	3181771	T	-	frameshift deletion	Protein of unknown function DUF4246
TWF1043	EYR41_005196	scaffold_3	1505468	1505468	-	TA	stop-gain	MFS transporter superfamily
TWF1046	EYR41_003064	scaffold_2	1780257	1780257	A	C	stop-gain	Velvet domain
TWF1046	EYR41_010493	scaffold_7	1849994	1849994	A	T	nonsynonymous SNV	Domain of unknown function DUF2183

387 References

- 388 1. Arai, T., Kasper, J.S., Skaar, J.R., Ali, S.H., Takahashi, C., and DeCaprio,
389 J.A.J.P.o.t.N.A.o.S. (2003). Targeted disruption of p185/Cul7 gene results in
390 abnormal vascular morphogenesis. *Proceedings of the National Academy of*
391 *Sciences* 100, 9855-9860.
- 392 2. Bolger, A.M., Lohse, M., and Usadel, B.J.B. (2014). Trimmomatic: a flexible
393 trimmer for Illumina sequence data. *Bioinformatics* 30, 2114-2120.
- 394 3. DiDonato, R.J., Arbuckle, E., Buker, S., Sheets, J., Tobar, J., Totong, R., Grisafi,
395 P., Fink, G.R., and Celenza, J.L.J.T.P.J. (2004). Arabidopsis ALF4 encodes a
396 nuclear-localized protein required for lateral root formation. *The Plant Journal* 37,
397 340-353.
- 398 4. Ellegren, H.J.T.i.e., and evolution (2014). Genome sequencing and population
399 genomics in non-model organisms. *Trends in ecology & evolution* 29, 51-63.
- 400 5. Gray, N.F. (1983). *Ecology of nematophagous fungi: Distribution and habitat.*
401 *Annals of Applied Biology* 102, 501-509.
- 402 6. Gulshan, K., Rovinsky, S.A., and Moye-Rowley, W.S.J.E.c. (2004). YBP1 and its
403 homologue YBP2/YBH1 influence oxidative-stress tolerance by nonidentical
404 mechanisms in *Saccharomyces cerevisiae*. *Eukaryot Cell* 3, 318-330.
- 405 7. Hsueh, Y.P., Gronquist, M.R., Schwarz, E.M., Nath, R.D., Lee, C.H., Gharib, S.,
406 Schroeder, F.C., and Sternberg, P.W. (2017). Nematophagous fungus *Arthrobotrys*
407 *oligospora* mimics olfactory cues of sex and food to lure its nematode prey. *eLife*
408 6.
- 409 8. Hsueh, Y.P., Mahanti, P., Schroeder, F.C., and Sternberg, P.W. *Current Biology*
410 (2013). Nematode-trapping fungi eavesdrop on nematode pheromones. *Curr Biol*
411 23, 83-86.
- 412 9. Li, H., and Durbin, R.J.b. (2009). Fast and accurate short read alignment with
413 Burrows–Wheeler transform. *Bioinformatics* 25, 1754-1760.
- 414 10. Li, H.J.a.p.a. (2013). Aligning sequence reads, clone sequences and assembly
415 contigs with BWA-MEM. *arXiv* :1303.3997 [q-bio.GN]
- 416 11. Li, H.J.B. (2011). A statistical framework for SNP calling, mutation discovery,
417 association mapping and population genetical parameter estimation from
418 sequencing data. *Bioinformatics* 27, 2987-2993.
- 419 12. Li, J., Wu, R., Wang, M., Borneman, J., Yang, J., and Zhang, K.-Q.J.F.b. (2019).
420 The pH sensing receptor AopalH plays important roles in the nematophagous
421 fungus *Arthrobotrys oligospora*. *Fungal biology* 123, 547-554.
- 422 13. Li, X., Kang, Y.-Q., Luo, Y.-L., Zhang, K.-Q., Zou, C.-G., and Liang, L.-M.J.J.o.M.
423 (2017). The NADPH oxidase AoNoxA in *Arthrobotrys oligospora* functions as an

- 424 initial factor in the infection of *Caenorhabditis elegans*. *Journal of Microbiology*
425 55, 885-891.
- 426 14. Lopez-Llorca, L.V., Maciá-Vicente, J.G., and Jansson, H.B. (2007). Mode of
427 Action and Interactions of Nematophagous Fungi. *In Integrated management and*
428 *biocontrol of vegetable and grain crops nematodes*. Springer, Dordrecht 2, 51-76.
- 429 15. Nordbring-Hertz, B., Jansson, H.-B., and Tunlid, A. (2011). Nematophagous fungi.
- 430 16. Poplin, R., Ruano-Rubio, V., DePristo, M.A., Fennell, T.J., Carneiro, M.O., Van
431 der Auwera, G.A., Kling, D.E., Gauthier, L.D., Levy-Moonshine, A., and Roazen,
432 D.J.B. (2017). Scaling accurate genetic variant discovery to tens of thousands of
433 samples. *bioRxiv*, 201178.
- 434 17. Russell, J.J., Theriot, J.A., Sood, P., Marshall, W.F., Landweber, L.F., Fritz-Laylin,
435 L., Polka, J.K., Oliferenko, S., Gerbich, T., and Gladfelter, A.J.B.b. (2017). Non-
436 model model organisms. *BMC biology* 15, 1-31.
- 437 18. Wang, K., Li, M., and Hakonarson, H.J.N.a.r. (2010). ANNOVAR: functional
438 annotation of genetic variants from high-throughput sequencing data. *Nucleic*
439 *Acids Research* 38, e164-e164.
- 440 19. Wang, R., Wang, J., and Yang, X. (2015). The extracellular bioactive substances
441 of *Arthrobotrys oligospora* during the nematode-trapping process. *Biological*
442 *Control* 86, 60-65.
- 443 20. Wu, B., Hussain, M., Zhang, W., Stadler, M., Liu, X., and Xiang, M.J.M. (2019).
444 Current insights into fungal species diversity and perspective on naming the
445 environmental DNA sequences of fungi. *Mycology* 10, 127-140.
- 446 21. Yang, C.T., Vidal-Diez de Ulzurrun, G., Goncalves, A.P., Lin, H.C., Chang, C.W.,
447 Huang, T.Y., Chen, S.A., Lai, C.K., Tsai, I.J., Schroeder, F.C., *et al.* (2020). Natural
448 diversity in the predatory behavior facilitates the establishment of a robust model
449 strain for nematode-trapping fungi. *Proceedings of the National Academy of*
450 *Sciences U S A*.
- 451 22. Youssar, L., Wernet, V., Hensel, N., Yu, X., Hildebrand, H.-G., Schreckenberger,
452 B., Kriegler, M., Hetzer, B., Frankino, P., and Dillin, A.J.P.g. (2019). Intercellular
453 communication is required for trap formation in the nematode-trapping fungus
454 *Duddingtonia flagrans*. *Plos Genetics* 15, e1008029.
- 455 23. Zhen, Z., Xing, X., Xie, M., Yang, L., Yang, X., Zheng, Y., Chen, Y., Ma, N., Li,
456 Q., Zhang, K.-Q.J.F.G., *et al.* (2018). MAP kinase Slt2 orthologs play similar roles
457 in conidiation, trap formation, and pathogenicity in two nematode-trapping fungi.
458 *Fungal Genetics and Biology* 116, 42-50.

459